

## **Use of the BT2 Water Line List to Determine the Rotational Temperature and H<sub>2</sub>O Column Density of the Circumstellar Envelope on Five Dates**

R. J. Barber

*University College London, WC1E 6BT, UK*

D. P. K. Banerjee

*Physical Research Laboratory, Navrangpura, Ahmedabad, India*

N. M. Ashok

*Physical Research Laboratory, Navrangpura, Ahmedabad, India*

J. Tennyson

*University College London, WC1E 6BT, UK*

**Abstract.** BT2 is the most accurate and complete synthetic water line list in existence; it includes over 505 million transitions. BT2 spectra generated at various temperatures and column densities were fitted to observed H band spectra of V838 Mon recorded on 5 dates between 20 Nov. 2002 and 25 Dec. 2004. Five absorption features in the observed spectra were identified as being due to water. With one exception, where there was a single strong water line, all of the features were blends of water lines. 17 individual water lines were assigned and the rotational temperatures and H<sub>2</sub>O column densities of the circumstellar ejected envelope were determined for each of the five dates.

### **1. The BT2 Line List**

The practical limitations on measuring experimentally the huge amounts of data that are required by astronomers analysing high resolution spectra or developing stellar atmospheric models, mean that these areas are largely dependent on ‘synthetic’, that is to say, computed, molecular spectra.

BT2 is a synthetic list of H<sub>2</sub><sup>16</sup>O transition frequencies and intensities (Barber et al. 2006). It was produced at UCL using a discrete variable representation two-step approach for solving the rotation-vibration nuclear motions (Tennyson et al. 2004). It is the most complete water line list in existence, comprising over 500 million transitions (65% more than any other list) and it is also the most accurate (over 90% of all known experimental energy levels are within 0.3 cm<sup>-1</sup> of the BT2 values). Its accuracy has been confirmed by extensive testing against astronomical and laboratory data.

The line list has already found application in a wide range of astrophysical environments. It has been used to identify individual water lines in: the spectra of comets (Barber et al., 2007), sunspots (Zobov et al. 2006), cool stars (Jones et

al. 2005) and brown dwarfs (Smith et al. 2003), as well as in V838 Mon (Banerjee et al. 2005). In a number of these cases physical parameters have been derived from the intensities of the lines. Practical applications of BT2 are not confined to the field of astronomy. The line list is now the preferred reference tool for many researchers engaged in the identification of water lines in high temperature laboratory torch spectra (Coheure et al. 2005; Zobov et al. 2006)

Although several other synthetic water line lists are used by astronomers, none of these is sufficiently complete or accurate to enable them to adequately reproduce the H<sub>2</sub>O spectral features observed at high resolution or to produce satisfactory results when included in models of cool stellar atmospheres (Jones et al. 2003). BT2 was developed to overcome these deficiencies and to provide astronomers with an accurate and versatile tool.

The data are in two parts. The first, the ‘Levels File’ is a list of 221 097 energy levels, ordered by rotation quantum number J and symmetry block. About 25 000 of these energy levels have been labelled with the appropriate angular momentum (J, K<sub>a</sub>, K<sub>c</sub>) and vibrational ( $\nu_1$ ,  $\nu_2$ ,  $\nu_3$ ) quantum numbers. An extract from the Levels File with an explanation of the contents of each of the columns in the file is given in Table 1. The second part of BT2 is the ‘Transitions File’. This has 505 806 202 entries. Each transition references upper and lower energy levels in the Levels File and gives the Einstein A<sub>if</sub> coefficient for the transition. An extract from the Transitions File is given in Table 2.

In uncompressed form the BT2 Transitions File is 12.6 Gb of data. Therefore, in order to facilitate use of the list, the transitions have been ordered by frequency and separated into 16 smaller files, each representing a specific frequency range. BT2 is available electronically in compressed form at <http://www.tampa.phys.ucl.ac.uk/ftp/astrodata/water/BT2/> and also at <ftp://cdsarc.u-strasbg.fr/cats/VI/119>

These ftp sites also include a Fortran program, spectra-BT2.f90, that will enable users to generate emission or absorption spectra from BT2 by specifying various parameters including: temperature, frequency range, cut-off intensity and line width. There is also a facility to generate spectra with ro-vibrational assignments if required.

Table 1. Extract from the BT2 Levels File. A: Row in file, B: J, C: Symmetry (1-4) D: Row in block, E: frequency in cm<sup>-1</sup> F, G, H:  $\nu_1$ ,  $\nu_2$ ,  $\nu_3$ . I, J, K: J, K<sub>a</sub>, K<sub>c</sub>. Reproduced from Barber et al. (2006).

A	B	C	D	E	F	G	H	I	J	K
2284	2	2	5	3885.718672	0	0	1	2	2	1
2285	2	2	6	4777.145956	0	3	0	2	1	1
2286	2	2	7	5332.258064	1	1	0	2	1	1
2287	2	2	8	5472.371851	0	1	1	2	2	1
2288	2	2	9	6254.694085	0	4	0	2	1	1
2289	2	2	10	6876.917089	1	2	0	2	1	1
2290	2	2	11	7027.396535	0	2	1	2	2	1
2291	2	2	12	7293.201639	2	0	0	2	1	1
2292	2	2	13	7376.617020	1	0	1	2	2	1
2293	2	2	14	7536.864373	0	0	2	2	1	1

Table 2. Extract from BT2 Transitions File. A, B: Row numbers in the Levels File. The identification of A as an upper level is not necessary because upper and lower can be indentified from Level(A) - Level(B). C:  $A_{if}$  ( $s^{-1}$ ). Reproduced from Barber et al. (2006).

A	B	C
1000	239	9.671E+01
1001	239	1.874E+00
1002	239	4.894E-03
1003	239	1.140E-04
1004	239	1.707E-02
1005	239	8.473E-08
1006	239	6.535E-04
1007	239	7.157E+00
1008	239	6.403E-06
1009	239	9.861E-05

## 2. Introduction to V838 Mon

V838 Mon was detected in eruption on 2002 January 6 by Brown (2002) with a peak amplitude of  $V_{max} = 10$ . Over the following two months there were two more outbursts with amplitudes  $V_{max} = 6.7$  and 7 respectively. In February 2002, the spectrum of V838 Mon resembled an F-type supergiant. However, it cooled rapidly and by early 2003 it had the spectral characteristics of a late M- or early L-type giant (Evans et al. 2003). The photospheric temperature of the star was estimated to be  $\sim 2100\text{K}$  and that of the envelope,  $\sim 800\text{K}$ .

Figs. 1 and 2 of Evans et al. (2003) and Figs. 6 and 7 of Lynch et al. (2004) reveal wide, deep absorption troughs between the spectral bands. These include the absorption features at  $1.4 \mu\text{m}$  between the *J* and *H* bands, and at  $1.9 \mu\text{m}$  between the *H* and *K* bands. These inter-band features are due to water and are commonly observed in cool M stars (Lançon & Rocca-Volmerange 1992). However, neither Evans et al. (2003) nor Lynch et al. (2004) recorded individual water lines, only broad features.

An expanding ‘light-echo’ was also seen around the star (Henden et al. 2002; Bond et al. 2003) and this was initially believed to be due to light that had been emitted during the recent brightenings being reflected from dust ejected by the progenitor star in previous epochs. However, the idea that the light echo is a reflection from interstellar dust whose origin is unconnected with V838 Mon (see for example Banerjee et al. 2007) is gaining popularity.

There are several theories regarding the nature of V838 Mon. Possibly we are observing an AGB object (these are known to be unstable with deep convective shells) throwing off material and rapidly evolving on the H-R diagram. The mechanism that would cause such a development is not understood. It could possibly be related to a B3 star observed in the same field.

Another theory involves the ingestion by an expanding giant of three planets, each event corresponding to one of the observed light peaks (Retter et al. 2007). Yet another proposal by Soker & Tylenda (2007) involves the merger of

a close binary pair. There is also uncertainty regarding the temperature of the progenitor. Tylenda, Soker, & Szczerba (2005) suggest an early B-type with a temperature of  $\sim 30\,000$  K.

It has been noted that the V838 Mon's outbursts and the star's subsequent evolution are similar to those of V4332 Sgr and M31-RV (both of these objects have erupted in the last 10-15 years) and that these three objects may represent a new class of eruptive variable (Banerjee & Ashok 2004).

### 3. Shell Temperature and $\text{H}_2^{16}\text{O}$ Column Density

We report here on the the manner in which we used the BT2 line list (Barber et al. 2006) to determine the temperature and  $\text{H}_2\text{O}$  column density of the recently-ejected circumstellar envelope on five dates between 20 Nov. 2002 and 25 Dec. 2004, first detailed in Banerjee et al. (2005).

Since early 2002, with the exception of the rainy season (mid-June to early October), near-IR spectra of V838 Mon have been recorded at fairly regular intervals using the 1.2m telescope on Mt. Abu. We examined five  $H$  band spectra, obtained at a resolving power of  $\sim 1000$ , between November 2002 and December 2004.

$H$  band spectra obtained by Banerjee et al. are shown in Fig. 1. Apart, from the absorption features longward of  $1.73\ \mu\text{m}$ , which we identify as being due to water, and the AIO bands that are indicated (Banerjee et al. 2003), most of the other strong features in Fig. 1 are due to the second overtone of  $^{12}\text{CO}$  (Banerjee & Ashok 2002)

By comparing the observed spectra with synthetic BT2 spectra we were able to identify a number of features in Fig. 1 as being due to water. The relative intensities of the various features are very temperature-dependent. By generating spectra at different temperatures and testing for best fit with observation, it can be seen from Fig. 2 that, within the errors shown in Table 4, it was possible to determine the temperature of the region within which absorption was taking place, on each of the five dates. It will be seen from Table 4 that between 19 November 2002 and 25 December 2004 the temperature of the water-absorbing region decreased from  $900\pm 30$  K to  $750\pm 50$  K, that is to say a reduction of  $150\pm 60$  K over a period of 767 days.

Many of the transitions within the BT2 line list have been labelled, and consequently it was possible to identify the 17 strong lines that comprise the five main absorption features in Fig. 2. The details are given in Table 3. The lower and upper levels for each of these transitions are labelled in the manner:  $(\nu_1\ \nu_2\ \nu_3)[J\ K_a\ K_c]$ , where the terms in round brackets are the vibrational quantum numbers, those in the square brackets represent the asymmetric top rotational quantum number and its projection onto two orthogonal axes (A and C) respectively. It will be seen that with the exception of one line at  $1.74454\ \mu\text{m}$  all of these strong transitions are in the (0 0 0)-(0 1 1) band.

Table 3 gives the relative intensities of the 17 strongest synthetic  $\text{H}_2\text{O}$  lines in the wavelength range  $1.726$  to  $1.751\ \mu\text{m}$  at a temperature of 800 K; it also gives the relative intensity of the five strong absorption features that are the result of the blending of these lines. The intensity is expressed as the total integrated line intensity within the bin whose position corresponds to that of maximum

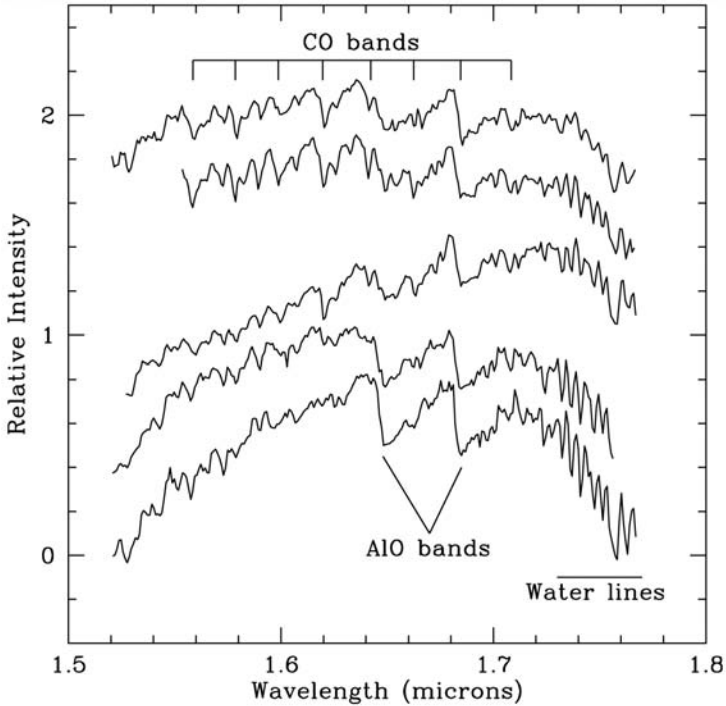


Figure 1. H band spectra of V838 Mon. The spectra are vertically offset by arbitrary amounts for clarity of presentation. Bottom to top, the dates are: 20 Nov. 2002, 25 Jan. 2003, 14 Dec. 2003, 15 Apr. 2004 and 25 Dec. 2004. Reproduced from Banerjee et al. (2005).

absorption within the feature. The apparent discrepancies between the two sets of data are explained by the fact that the features comprise not only the strong lines listed in Table 3, but a large number of weak lines that can collectively make an important contribution to total absorption. Lastly, it is possible to estimate the H<sub>2</sub>O column densities using  $I = I_0 \exp(-\kappa_\lambda NS)$ , where  $N$  is the number of water molecules per cm,  $S$  is the distance in cm and the product  $NS$  is the column density (molecules  $\text{cm}^{-2}$ ).  $\kappa_\lambda$  is the opacity at wavelength  $\lambda$  and is one of the outputs of the program spectra-BT2.f90. Once the best temperature fit has been established, the optimum values of  $I_0$  and  $NS$  that give the best fit to the observed data were obtained. The effect of increasing  $I_0$  is to raise the overall level of the synthetic plot, whilst increasing  $NS$  has the effect of increasing the depth of the strong absorption features relative to the weak ones. Table 4 details our estimates of column density on each of the five dates. We believe that our methodology is liable to suffer from systematic errors and consequently we estimate the errors as being +100%, -50%. However, the comparison between the column densities at the different dates will be more accurate, and we estimate the error in the relative numbers at +25%, -20%.

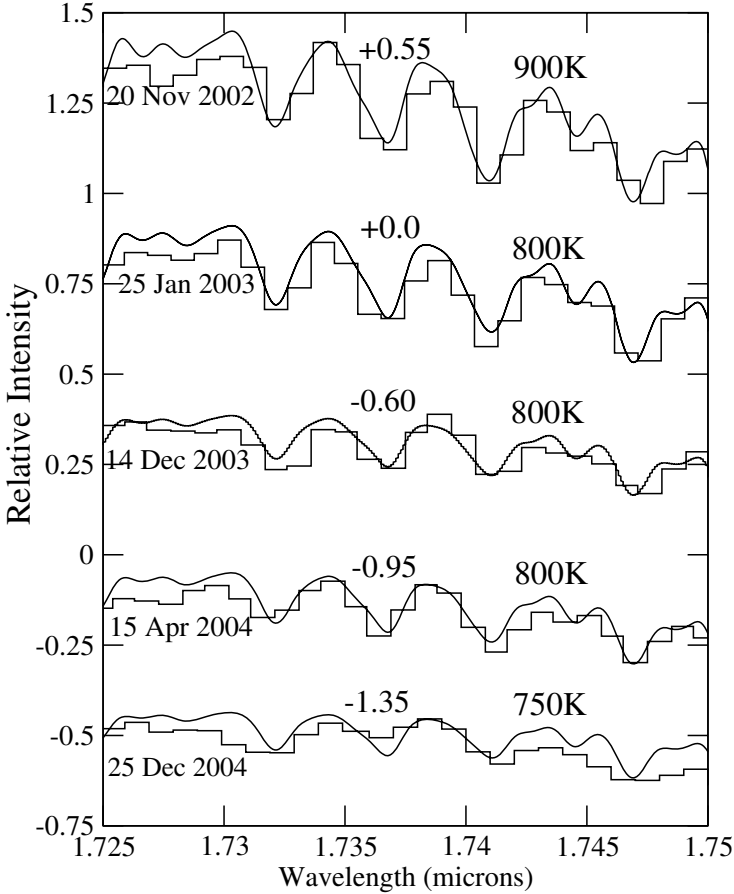


Figure 2. Synthetic spectra (solid curves) superimposed on the observed data (histograms), for the different epochs of observation. For ease of presentation, the five pairs of data are plotted with constants added to their relative intensities. The values of these offsets are listed next to the plots. Reproduced from Banerjee et al. (2005).

### 3.1. Discussion

We have compared our column density and temperature estimates with those derived by Lynch et al. (2004). The envelope temperature of  $800 \pm 30$  K on 25 January 2003 is consistent with that of 750-790 K derived by Lynch et al. (2004) at a similar date and based on observations of  $\text{H}_2\text{O}$ , CO molecular bands and the  $\text{SiO}(\nu_2)$  feature. Our estimate of the  $\text{H}_2\text{O}$  column density on 25 January 2003 is approximately half the Lynch et al. (2004) value, but the figures are in agreement within our estimated error.

Even though the rate of cooling must slow, it is likely that at some future time the temperature of the water-bearing envelope will reach the ice sublimation temperature ( $\sim 150\text{K}$ ) to form water-ice. Such a development would further

Table 3. Line Centres and Relative Intensities of lines  $I_{line}$  and features  $I_{fea.}$ , computed at 800 K, for 25 Jan 2003. Reproduced from Banerjee et al. (2005).

Lower level ( $\nu_1\nu_2\nu_3$ )[JK <sub>a</sub> K <sub>c</sub> ]	Upper level ( $\nu_1\nu_2\nu_3$ )[JK <sub>a</sub> K <sub>c</sub> ]	$\lambda$ $\mu\text{m}$	$I_{line}$ Rel.	Center $\mu\text{m}$	$I_{fea.}$ Rel.
(0 0 0)[7 3 4]	(0 1 1)[8 5 3]	1.73202	1.93	1.7329	1.77
(0 0 0)[6 3 4]	(0 1 1)[7 5 3]	1.73239	1.61		
(0 0 0)[9 2 7]	(0 1 1)[10 4 6]	1.73686	2.83	1.73686	1.93
(0 0 0)[15 7 8]	(0 1 1)[16 7 9]	1.73987	1.23	1.74071	2.21
(0 0 0)[15 5 10]	(0 1 1)[16 5 11]	1.74036	2.07		
(0 0 0)[16 6 11]	(0 1 1)[17 6 12]	1.74082	1.03		
(0 0 0)[15 6 9]	(0 1 1)[16 6 10]	1.74121	1.91		
(0 0 0)[5 3 2]	(0 1 1)[6 5 1]	1.74128	1.26		
(0 0 0)[14 8 7]	(0 1 1)[15 8 8]	1.74269	1.27		
(0 0 0)[7 0 7]	(0 1 1)[8 2 6]	1.74445	1.24	Shoulder	1.36
(0 0 0)[13 5 8]	(1 1 0)[14 6 9]	1.74454	1.23	1.74456	1.77
(0 0 0)[13 9 4]	(0 1 1)[14 9 5]	1.74471	1.12		
(0 0 0)[14 7 8]	(0 1 1)[15 7 9]	1.74650	2.12	1.74688	2.59
(0 0 0)[6 2 5]	(0 1 1)[7 4 4]	1.74674	2.29		
(0 0 0)[16 5 12]	(0 1 1)[17 5 13]	1.74680	1.50		
(0 0 0)[8 2 6]	(0 1 1)[9 4 5]	1.74728	1.36		
(0 0 0)[14 6 8]	(0 1 1)[15 6 9]	1.74750	1.13		

Table 4. Temperature and Column Densities. Reproduced from Banerjee et al. (2005).

Obs. Date	Temperature (°K)	Error (°K)	Column Density mols cm <sup>-2</sup>
20 Nov 2002	900	30	9.3x10 <sup>21</sup>
25 Jan 2003	800	30	9.0x10 <sup>21</sup>
14 Dec 2003	800	30	3.8x10 <sup>21</sup>
15 Apr 2004	800	40	5.1x10 <sup>21</sup>
25 Dec 2004	700	50	4.6x10 <sup>21</sup>

enhance the similarity between V838 Mon and its possible analog V4332 Sgr in which water ice was detected strongly 10 years after the object's outburst (Banerjee & Ashok 2004).

**References**

- Banerjee, D.P.K., & Ashok, N.M. 2002, *A&A*, 395, 161
- Banerjee, D.P.K., Varricatt, W.P., Ashok, N.M., & Launila O. 2003, *ApJ*, 598, L31
- Banerjee, D.P.K., & Ashok, N.M. 2004, *ApJ*, 604, L57
- Banerjee, D.P.K., Barber, R.J., Ashok, N.M., & Tennyson J. 2005, *ApJ*, 627, L141
- Banerjee, D.P.K., Su, K.Y.L., Misselt, K.A., & Ashok, N.M. 2006, *ApJ*, 644, L57
- Barber, R.J., Tennyson, J., Harris, G.J., & Tolchenov, R. 2006, *MNRAS*, 368, 1087
- Barber, R.J., Miller, S., Stallard, T., Tennyson, J. et al. 2007, *Icarus*, in press
- Bond, H.E., Henden, A.A., Levay, Z.G., et al. 2003, *Nature*, 422, 405
- Brown, N.J. 2002, *IAU Circ*, 7785
- Coheur, P.-F., Bernath, P.F., Caleer, M., Colin, R., et al. 2005, *J. Chem. Phys.*, 122, 074307
- Evans, A., Geballe, T.R., Rushton, M.T., Smalley, B., et al. 2003, *MNRAS*, 343, 1054
- Henden, A.A., Munari, U., & Schwartz, M. 2002, *IAU Circ.*, 7859
- Jones, H.R.A., Pavlenko, Y., Viti, S., & Tennyson, J. 2003 'Proceedings of 12th Cambridge Workshop on Cool Stars', eds Brown A., Harper G.M., Ayres T.R., p. 899
- Jones, H.R.A., Pavlenko, Y., Viti, S., Barber, R.J., et al. 2005, *MNRAS*, 358, 105
- Lançon, A., & Rocca-Volmerange, B. 1992, *A&AS*, 96, 593
- Lynch, D.K., Rudy, R.J., Russell, R.W., Mazuk, S., et al. 2004, *ApJ*, 607, 460
- Retter, A., Zhang, B., Siess, L., & Levinson, A. 2007, *MNRAS*, submitted
- Smith, V.V., Tsuji, T., Hinkle, K.H., Cunha, K., et al. 2003, *ApJ*, 582, L105
- Soker, N., & Tylenda, R. 2007, in *The Nature of V838 Mon and its Light Echo*, R.L.M. Corradi & U. Munari eds., ASP Conf. Ser. 363, 280
- Tennyson, J., Kostin, M., Barletta, P., Harris, G.J., Poyansky, O.L., et al. 2004, *Comp. Phys. Comm.*, 163, 85
- Tylenda, R., Soker, N., & Szczerba, R. 2005, *A&A*, 441, 1099
- Zobov, N.F., Shirin, S., Polyansky, O.L., Barber, R.J., et al. 2006, *J. Mol. Spec.*, 237, 115